Proc. Natl. Acad. Sci. USA
Vol. 82, pp. 386–390, January 1985
Biophysics

Light-harvesting chlorophyll *a*/*b*–protein: Three-dimensional structure of a reconstituted membrane lattice in negative stain

(image reconstruction/photosynthesis/integral membrane protein/two-dimensional crystal/thylakoid stacking)

JADE LI†

Department of Biochemistry, Columbia University, New York, NY 10032

Communicated by Daniel Branton, March 19, 1984

ABSTRACT **The three-dimensional structure of a negatively stained hexagonal membrane lattice containing the light-harvesting chlorophyll *a*/*b*–protein complex and phospholipids has been determined to 30-Å resolution by image reconstruction from electron micrographs. This lattice has *p*321 symmetry, a lattice constant of 125 Å and a thickness of 75 Å. The monomer is shown to be an elongated molecule about 65 Å long in the dimension perpendicular to the plane of the membrane. It spans the hydrophobic domain of the membrane in an asymmetric fashion, projecting ≈20 Å from one surface and less from the other. On the basis of this image and available biochemical data, the structure of the complex in the native thylakoid membrane is proposed.**

The light-harvesting chlorophyll *a*/*b*–protein complex (LHC) is the major integral protein of chloroplast thylakoid membranes, making up about half the protein weight as well as half the chlorophyll weight in these membranes (1). It serves a dual function as the major antenna pigment for photosynthesis and the thylakoid stacking factor (2). The holoprotein contains noncovalently bound chlorophylls *a* and *b* in roughly equal amounts (1).

In thylakoid membranes of the pea, two forms of LHC apopolypeptides of very similar molecular weights, p15 and p16, have been identified by gel electrophoresis; the larger, p15, is predominant (3, 4). Genes for two variants of p15 have been sequenced (5, 6). They encode mature polypeptides of 233 amino acids that differ at 5 residues and have molecular weights of 25,000 and 25,013. In spite of the sequence heterogeneity even within p15, the p15 and p16 polypeptides were found to be structurally related (4) and, moreover, to show a degree of structural similarity with LHC polypeptides in other species—e.g., spinach, barley, and *Chlamydomonas reinhardii* (7, 8).

As the stacking factor, LHC is exposed on the outer thylakoid surface. Studies of thylakoid development imply that LHC is a constituent of the 140-Å-diameter, intramembrane particles (9), which in freeze–fracture and freeze–etch electron micrographs appear to span the thylakoid membrane (10). Antigenic sites on LHC were shown to be accessible from both membrane surfaces (11). However, no direct visualization of the three-dimensional structure of LHC in the membranes has been possible, owing to the complex composition of thylakoid membranes.

LHC can be solubilized from pea thylakoid membranes under nondenaturing conditions (12). The purified protein has been incorporated into phospholipid vesicles and induced to crystallize in the plane of the lipid bilayer (13–16). Using x-ray diffraction and electron microscopy, Li and Hollingshead (16) showed that LHC lattices in the reconstituted membranes are hexagonal, with a lattice constant of 125 Å and a thickness of 70 Å. There is a 2-fold axis in the membrane plane, indicating bidirectional insertion of LHC molecules. Kühlbrandt *et al.* (17) reported that a hexagonal lattice formed by LHC and Triton X-100 without addition of lipids has the same planar lattice constant of 125 Å but a smaller thickness of 40–50 Å. This lattice has *p*321 symmetry (17, 18).

In this study, the LHC lattices have been isolated from the reconstituted membranes (16) by eliminating the contiguous pure lipid phase. The three-dimensional structure of the lattice in negative stain has been determined by image reconstruction from electron micrographs (28, 30).

METHODS

Biochemical Procedures. LHC was isolated from pea (*Pisum sativum*, var. Progress No. 9) seedlings (12) and stored at −80°C, at 5–8 mg/ml in 10 mM Tricine [*N*-tris(hydroxymethyl)methylglycine], pH 7.8/1.5% (vol/vol) Triton X-100/10 mM KCl/3 mM NaN_3. Protein (19, 20) and chlorophyll (21) were determined using the above storage buffer as the blank. Protein purity was established by $LiDodSO_4$/PAGE at 4°C.

Lecithin was prepared from egg yolks (22) and stored in absolute ethanol at −196°C. The lecithin migrated as a single spot on silica-gel TLC plates developed with $CHCl_3/CH_3OH/H_2O$ (65:25:4, vol/vol). Only fractions having an oxidative index (23) of fatty acyl chains <0.2 were used for reconstitution. Lipid concentration was measured by phosphate assay (24).

LHC was incorporated into single-walled lecithin vesicles (25) by freezing and thawing as described (14, 16). The lipid control was prepared by substituting the storage buffer containing Triton X-100 for LHC; the protein control, by substituting 18 mM sodium phosphate, pH 8.0, for the lipid vesicles. Excess Triton X-100 was removed by gentle stirring for 2 hr at 4°C with a 167-fold weight excess of washed Bio-Beads SM-2 (26, 27). After removing the beads by centrifugation, $MgCl_2$ was added to 2 mM to induce crystallization.

The reconstitution products were fractionated on a 12-ml 0–40% (wt/vol) sucrose density gradient in 10 mM Tricine, pH 7.8/2 mM $MgCl_2$/0.03% (vol/vol) Triton X-100/3 mM NaN_3/1 mM *N*-α-*p*-tosyl-L-lysine chloromethyl ketone/1 mM phenylmethylsulfonyl fluoride. Triton X-100 was included to solubilize the pure lipid phase contiguous with the LHC lattices (16). After centrifugation at 39,000 rpm in the Beckman SW41 rotor for 20 hr at 4°C, 200-μl fractions were collected. The sucrose concentration (and, hence, buoyant density) of each fraction was measured by refractometry. Duplicate aliquots from the fractions were assayed for protein (20) and chlorophyll (21) and then for lipid phosphate

The publication costs of this article were defrayed in part by page charge payment. This article must therefore be hereby marked "*advertisement*" in accordance with 18 U.S.C. §1734 solely to indicate this fact.

Abbreviation: LHC, light-harvesting chlorophyll *a*/*b*–protein complex.

†Present address: Medical Research Council Laboratory of Molecular Biology, Hills Rd., Cambridge CB2 2QH, England.

(24) after extraction into $CHCl_3/CH_3OH$ (2:1, vol/vol) to remove sucrose and inorganic phosphate. Adjacent fractions with the same protein/lipid ratio were combined for examination by electron microscopy and x-ray diffraction. The protein composition of the fractions was examined by gel electrophoresis (3).

Density gradients were also prepared from Percoll (Pharmacia) solutions in 10 mM Tricine, pH 7.8/2 mM $MgCl_2$/3 mM NaN_3, with or without 0.03% (vol/vol) Triton X-100. Samples were mixed into the solution and centrifuged in the MSE 10 × 10 ml rotor at 25,000 × g_{av} for 5 hr at 5°C. The density of each band was determined from the weight of a 100-μl aliquot.

Electron Microscopy and Image Reconstruction. Sucrose was removed from gradient fractions by dialysis against washing buffer [10 mM Tricine, pH 7.8/2 mM $MgCl_2$/0.03% (vol/vol) Triton X-100/3 mM NaN_3]. Alternatively, the fractions were diluted in washing buffer, and the lattices or vesicles were collected by centrifugation. The sample was applied to grids in washing buffer and negatively stained with 2% uranyl acetate.

Images were recorded at ×33,000–43,000 magnification using a Philips EM400 microscope operated at 80 kV. Using a 60°-tilt goniometer stage modified by J. F. Deatherage, multiple images of the same specimen area were recorded at 5° tilt intervals beginning at the maximum tilt angle. Focusing and compensation for astigmatism were performed on adjacent areas. Untilted images were recorded at the start and end of each tilt series; if comparison of their optical diffraction patterns indicated significant degradation, the series was rejected.

Image areas suitable for processing were selected by optical diffraction (28). In addition, areas containing multilayered lattices were rejected for three-dimensional reconstruction but were used for computing untilted filtered projections. The images were scanned on a flatbed microdensitometer (29) in 512 × 512 rasters at 20-μm intervals, corresponding at ×33,000 magnification to a square specimen area 0.3 μm on a side, sampled at 6-Å intervals.

Fourier transforms of the series of tilted images were combined to form a three-dimensional data set of amplitudes and phases along the lattice lines (28, 30, 31). Phase residuals calculated under different two-sided plane groups were compared to determine the symmetry of the structure. On each lattice line, a continuous curve of structure factors was obtained by interpolation followed by real-space filtration (32). Fourier inversion led to the three-dimensional map of the structure.

The lattice constant was measured on x-ray powder patterns from pellets of the membrane lattices. CuKα rays from an Elliot GX13 rotating anode were focused by double mirrors; the specimen was 42 cm from the film.

RESULTS

Density Gradient Analyses. In the sucrose gradients containing 2 mM $MgCl_2$ and 0.03% Triton X-100, the lipid and protein controls for the reconstitution had buoyant densities of 1.04 g/ml and 1.13 g/ml, respectively. The reconstituted membrane lattices fractionated into a "light" band at 1.08 g/ml and a "heavy" band at 1.11 g/ml. The light band contained protein and lipid at a weight ratio of 1.46 ± 0.35 (see *Methods*), corresponding to a molar ratio of about 1:20, calculated using molecular weights of 25,000 for the LHC protein and 850 for egg lecithin. In the heavy band, the protein/lipid ratio was 3.82 ± 0.73 by weight (1:8 molar ratio). Using these ratios as weighting factors, the buoyant densities of the lattice bands were found to equal the weight average of those of the controls on the same gradient.

The polypeptide composition of the light and heavy lattice fractions and of the protein control appeared identical on $LiDodSO_4$/PAGE. Both the major and minor LHC polypeptides, p15 and p16 (4), were found to have crystallized in the reconstituted membrane lattices. The protein/chlorophyll weight ratio was indistinguishable for the two lattice fractions and for the LHC control. This ratio, 2.96 ± 0.27, yields a stoichiometry of >10 chlorophylls per 25,000 daltons of polypeptide. The chlorophyll a/b ratio was 1.16 ± 0.09 in all these samples.

X-ray diffraction showed that the light and heavy lattices had the same lattice constant. When reconstituted lattices were formed from a starting protein/lipid weight ratio of 2:1 (1:15 molar ratio), about equal amounts of LHC were found crystallized in the light and in the heavy lattices. Pellets of membrane lattices from the heavy band alone or from the two bands combined gave rise to x-ray powder rings that index on a single hexagonal series of lattice constant 124.7 ± 0.3 Å. (Equality of lattice constant was also indicated by the reciprocal lattice parameters extracted from computed transforms of electron images of the lattices.) No lamellar reflection from a separate lipid phase was detected in these x-ray patterns. Since the lattice constant of LHC lattices that were contiguous with a pure lipid phase was determined to be 125 Å (16), this result shows that removal of excess lipid did not reduce the lattice constant.

When the heavy band from the sucrose gradient was recentrifuged in density gradients formed with a 40, 60, or 80% (wt/vol) Percoll solution, it equilibrated as a single green band at 1.030 ± 0.003 g/ml. The lower buoyant density in Percoll compared to that in sucrose can be explained if the repeating unit of the lattice contains a solvent-accessible space that excludes Percoll (diameter, 300 Å) but admits sucrose.

Electron Microscopy. All bands resolved in the sucrose density gradients were examined by electron microscopy after negative staining. The lipid control consisted of single-walled vesicles (Fig. 1*a*). The protein control showed hexagonal arrays that were only 3–4 unit cells across and poorly ordered, giving only the (1,0) and occasionally the (1,1) spots on optical diffraction.

The light fraction of reconstituted lattices contained hexagonal lattices up to 2 μm across (Fig. 1*b*). Different patches were stained to varying degrees of contrast, starting from minimal contrast. On the other hand, lattices in the heavy fraction always showed high contrast, which can be attributed to two effects: First, the areas around the intersection of 3-fold and 2-fold axes (see below) were well stained. In fact, stain density in this region was comparable to that along the borders of the lattice patch. Second, the heavy lattices consisted of multilayers stacked in register. The optical diffraction patterns of their tilt series revealed an interference effect due to the stacking—i.e., the intensities varied rapidly along individual lattice lines.

The interference effect renders multilayered specimens unsuitable for three-dimensional image reconstruction, unless the transform of the single layer can be recovered through oversampling of the lattice lines (33). The light fraction contained single-layered lattices. However, because of the variability of contrast among these lattices, the reconstruction was based on a single 12-member tilt series taken from a single specimen area.

Image Reconstruction. Optical diffraction from images of untilted lattices extends to the (3,1) order at 30-Å resolution in the plane, and shows $p6m$ symmetry in intensities. Phase residuals were evaluated from computed transforms in the possible two-sided plane groups. For 13 different untilted images, the residuals averaged 21.44° ± 11.39° in $p321$, 22.19° ± 10.58° in $p6$, 22.23° ± 10.53° in $p622$, 25.46° ± 13.18° in $p3$, and 25.51° ± 12.17° in $p312$. Therefore, at 30-Å

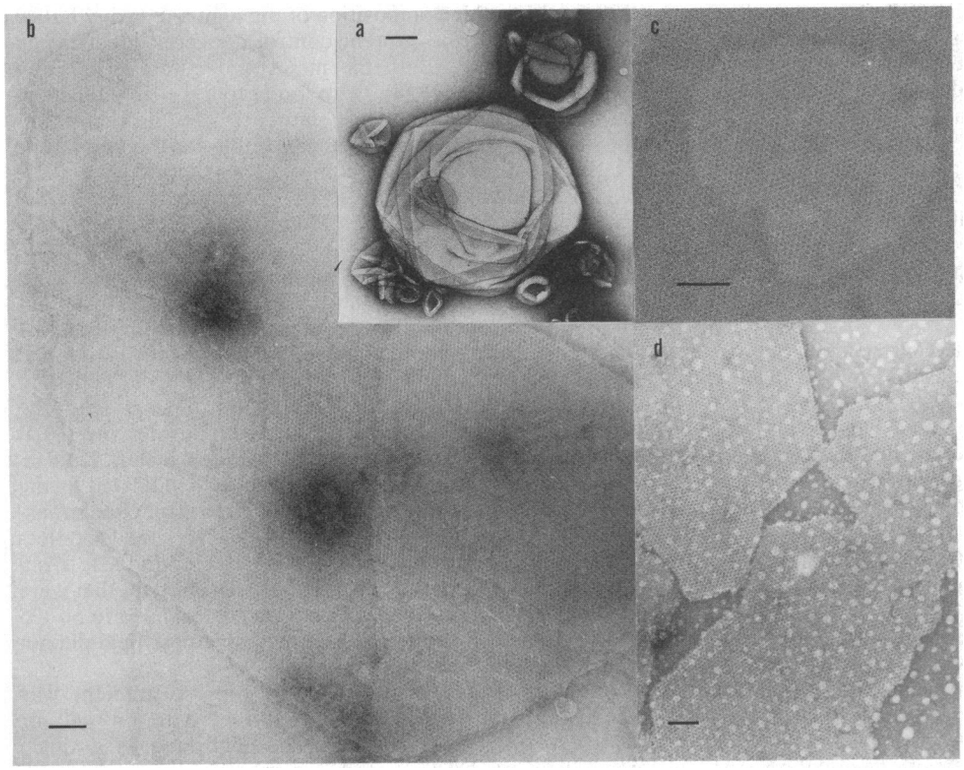

FIG. 1. Electron micrographs of (*a*) single-walled vesicles in the lipid control prepared by substituting a buffer containing Triton X-100 for LHC in the reconstitution; (*b*) LHC membrane lattices, 2 μm across, recovered from the sucrose gradient at 1.08 g/ml; (*c*) a single-layered LHC lattice surrounded by multilayered areas; and (*d*) multilayered LHC lattices recovered at 1.11 g/ml. (Bar = 1000 Å.)

resolution, *p*321 symmetry appeared to be favored (see *Discussion*).

For the lattice area imaged for the three-dimensional reconstruction, the phase residual of the tilt series was 7.95° ± 3.54° in *p*3, 11.31° ± 5.32° in *p*321, 17.42° ± 7.02° in *p*6, and 21.20° ± 10.73° in *p*622. These values indicate *p*3 or *p*321 symmetry. However, x-ray diffraction and freeze–fracture electron microscopy have shown that a 2-fold axis is contained in the lattice plane (14–17). In the negatively stained lattices, the slightly poorer agreement with *p*321 symmetry as compared to *p*3 is probably due to contact of one lattice surface with the carbon substrate, causing unequal staining of the two surfaces and the distortion of projecting structural elements on the contact surface. Therefore, the reconstruction was calculated in *p*321.

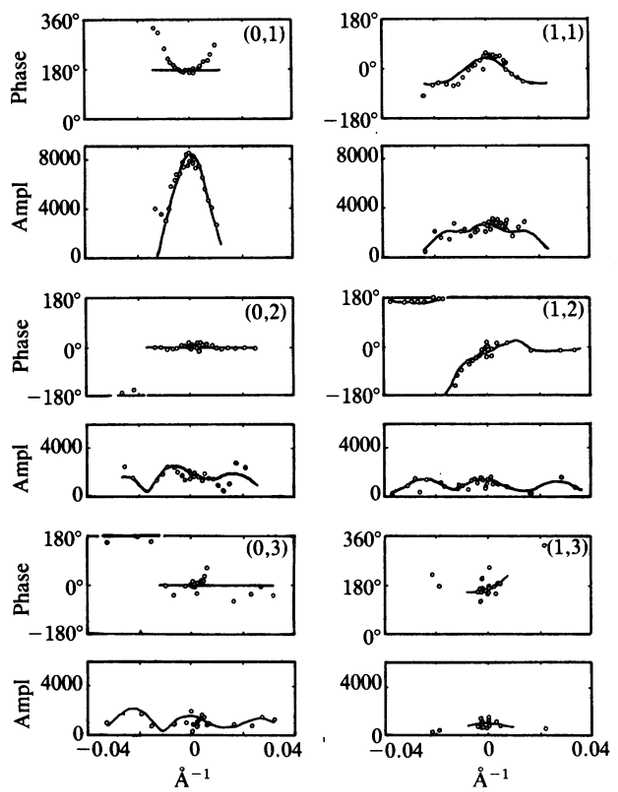

FIG. 2. Amplitudes (Ampl) and phases of structure factors along lattice lines (*h*, *k* given in parentheses) in *p*321 (see text).

Fig. 2 shows the amplitudes and phases along lattice lines in *p*321. That the observed phases on the (0,1) line deviate

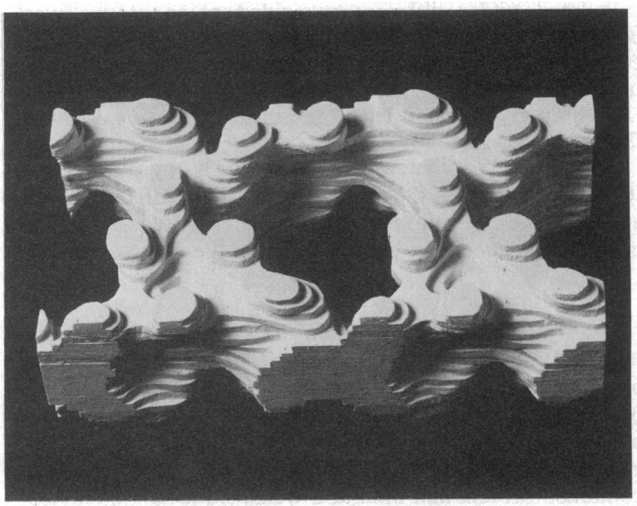

FIG. 3. Three-dimensional model representing the stain-excluding structures in the LHC lattice. The 20-Å-high surface protrusions due to LHC are grouped into two sorts of trimers, and each protrusion in one trimer forms a dimer with an adjacent protrusion in another trimer. Densities of the LHC molecules continue into the lattice interior forming a 35-Å-thick middle section of stain-exclusion, which is perforated by stain infiltration of the lipid area.

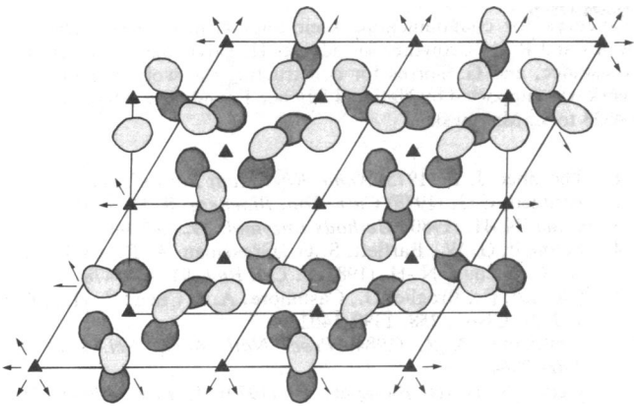

FIG. 4. Relationships of the rectangular area included in the model (see Fig. 3) to the unit-cell boundaries and symmetry elements of the $p321$ lattice. LHC molecules projecting on the upper and lower surfaces are, respectively, indicated in light and dark shading.

from the real with increasing tilt angle and that structure factors on the (1,1) line are centrosymmetric but about a point in z^* displaced from the origin are both indicative of the deviations from strict 2-fold symmetry about the in-plane axes already discussed. These effects have been corrected for in the symmetrized structure factors. Amplitudes along the (0,1) line are unaffected by the deviation, and they can be estimated to reach zero at about 70-Å z-spacing. By analogy with the transform of a rectangular slit, this implies a 70-Å average thickness for the LHC lattice. Furthermore, the calculated Fourier map shows density fluctuations above the noise level only within a central slab of 70–75 Å thickness. These results indicate that the structure imaged is only one membrane thick, confirming the lattice thickness measured by meridional x-ray diffraction from oriented, stacked LHC lattices (16).

The Three-Dimensional Model. The stain-excluding structures in the Fourier map are represented by the three-dimensional model shown in Fig. 3. The relationships of the rectangular area covered by the model to the unit-cell boundaries and the symmetry axes of the $p321$ planar lattice are diagrammed in Fig. 4.

The model shows that, within the unit cell (see Fig. 4) of 125-Å lattice constant, there are two sets of protruding trimers on each lattice face. These represent projecting domains of LHC molecules and are ≈26 Å in diameter. The center-to-center distance between protrusions in one set of trimers is ≈44 Å, and in the other, ≈46 Å. Distance between adjacent protrusions from two different trimers is ≈40 Å. These trimer and dimer interactions build up an extended lacework. Operation of the 2-fold axes in the plane brings trimers on opposite faces into a nearly staggered confirgura-

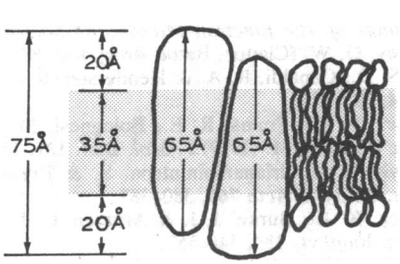

FIG. 5. Diagram illustrating the asymmetric placement of the LHC monomer relative to the hydrophobic domain (stippled area) of the reconstituted membrane. Molecular boundaries in the hydrophobic region are not determined at the 30-Å resolution, but are drawn schematically.

tion. Therefore, in projection the stain-excluding features of the lattice have a braided appearance. At the intersection of 3-fold and 2-fold axes, a hole ≈92 Å in diameter represents stain infiltration.

Side view of the model shows a 35-Å-thick middle band of stain exclusion, which probably corresponds to the hydrophobic domain of the membrane lattice. Protruding LHC molecules extend beyond this domain by 20 Å at most, giving the lattice a total thickness of 75 Å (Fig. 5).

DISCUSSION

Symmetry. The structure of the LHC membrane lattice determined in this study has $p321$ symmetry, as shown by phase relations in its three-dimensional transform at 30-Å resolution. The earlier report of $p622$ symmetry (16) was inconclusive, as it was based on $p6m$ symmetry of intensities in the ($hk0$) section, which is equally consistent with $p321$ or $p312$ symmetry.

Several lattice areas that were examined untilted in this study gave two-dimensional transform phases supporting $p622$ symmetry, whereas others indicated $p321$ symmetry. It is conceivable that sheet crystals of LHC can be obtained in either symmetry arrangement. The three-dimensional model (Fig. 3) suggests that a twist of one set of trimer about its 3-fold axis would result in $p622$ symmetry for the lattice. Thus, from the three-dimensional data at the present resolution, whether the structure is calculated in $p321$ symmetry (as was done on the basis of comparison of phase residuals) or in $p622$ symmetry, the resultant protein- and lipid-packing would not be substantially different. Alternatively, the $p622$ symmetry seen in projection was only apparent. This could be due to twinning of $p321$ lattices by a 180° rotation about an axis parallel to their 3-fold axes or, if the area imaged comprised stacked lattices, due to the superposition of two 3-fold symmetric lattices that are related by a 60° rotation.

Protein Content. The unit cell of the $p321$ lattice contains 6 asymmetric units and therefore must contain multiples of 6 LHC monomers. The lattice constant of 125 Å and average thickness of 70 Å give a unit-cell volume that is sufficient to accommodate 12 LHC monomers. In the Fourier map, stain-excluding structures occupy, on the average, 6887 Å^2 per unit cell in the lattice interior. If 12 monomers share this area, each will have an equivalent circular diameter of 27 Å, which is close to the 26 Å diameter of the surface protrusions. Such a cross-section compared to the volume expected for the monomer including bound chlorophylls implies an elongated shape, ≈65 Å long perpendicular to the membrane lattice. The stain-excluding volume of the unit cell is consistent with 12 monomers of this shape, but cannot be accounted for by only 6 monomers. Because of their thickness and strong surface relief, the stain-excluding structures are not likely due to lipid components of the lattice. Therefore, the asymmetric unit of the $p321$ lattice contains a noncrystallographic dimer of LHC molecules.

The noncrystallographic dimer does not correspond to a one-to-one complex of the LHC polypeptides p15 and p16, because p15 is predominant over p16 in the lattices as in the thylakoids. In view of the structural similarity among LHC polypeptides (4, 7, 8) and the sequence microheterogeneity within p15 (6), it is likely that they crystallize interchangeably in these lattices.

Lipid Content. Lipids in the light lattices probably form a bilayer over an area ≈92 Å in diameter and bounded by trimer and dimer clusterings of LHC. This area can accommodate ≈220 lipid molecules in a bilayer configuration, which agrees within experimental error with the lipid content of the unit cell calculated for 12 LHC monomers. The lipids appear to exchange with detergent, which was used for

dissolving the pure lipid phase outside the lattice patch and in sample application to the grid. The exchange facilitates stain infiltration of the lipid area, an effect observed in other sheet crystals of membrane proteins prepared with detergents (34).

In the heavy lattices, the protein/lipid ratio suggests that half of the lipids required for a continuous bilayer was replaced by detergent. The buoyant density of these lattices is lower in Percoll than in sucrose, consistent with the formation of a Percoll-excluding space as a result of the replacement.

Protein Packing. That the heavy and light lattices, which differ in lipid content, should have the same lattice constant suggests that the LHC lattices are stabilized by protein–protein interactions. It is reasonable to assume that the 12 prominent surface protrusions correspond to the 12 monomers and to the same polypeptide segments in each monomer. Therefore, the trimer and dimer interactions observable from the lattice surface occur between subunits in the same orientation with respect to the membrane plane. These interactions may also occur in the native thylakoid membrane. In addition, LHC subunits in the opposite orientations form lateral contacts in the hydrophobic interior of the membrane lattices. The latter interactions have no parallel in the natural membrane, where proteins are vectorially inserted.

Chlorophyll Protein Organization. Assays on the LHC lattices indicate that >10 moles of chlorophylls *a* and *b* are bound per polypeptide. A 25,000 M_r polypeptide cannot form a β-barrel that both encloses all the chlorophylls and conforms to the elongated shape indicated by image reconstruction. Therefore, the pigment/protein organization in this integral membrane protein must be different from that observed in the water-soluble bacteriochlorophyll *a* protein (35). Recent findings from circular dichroism and infrared linear dichroism (36), which show 44% of the LHC polypeptide in α-helical conformation and the helices in a predominantly transmembrane orientation, concur with this deduction.

Monomer Asymmetry. Image reconstruction of the reconstituted membrane lattice shows that the LHC monomer is an elongated structure about 65 Å long normal to the membrane plane; it spans the 35-Å-thick hydrophobic section of the membrane lattice in an asymmetric fashion, projecting 20 Å on one side and less on the other. Fig. 5 illustrates the asymmetric placement of the LHC monomer relative to a membrane bilayer. It is known that trypsin cleavage of 2000 daltons from the LHC polypeptide *in situ* reduces the capacity of thylakoids to stack (37). The sequence of the excised segment (38) matches the NH_2-terminal sequence of the major LHC polypeptide (5), thereby placing the NH_2 terminus on the outer thylakoid surface. A hydropathy plot (39) reveals that the NH_2-terminal 60 residues of the 233-residue LHC polypeptide are predominantly hydrophilic. Thus, it is possible that the NH_2-terminal quarter of the sequence is largely contained in the 20-Å protrusion seen in the reconstructed image. *In vivo* this domain would be oriented toward the outside of the thylakoids and contribute to thylakoid stacking. This orientation would explain the ability of reconstituted membrane lattices to mimic thylakoid stacking (14–17).

I am grateful to Dr. Richard Henderson for his guidance and encouragement of the three-dimensional reconstruction, Dr. T. S. Baker for computing the first filtered image, Drs. C. J. Arntzen and B. W. Matthews for helpful discussions, Drs. J. Breton and E. Nabedryk for communicating their unpublished results, Drs. L. Amos and R. A. Crowther for advice, H. Doyle and G. Vigers for assistance, and G. Torres for constructing the wood model. This work was supported by National Science Foundation Grant PCM81-04323 to L. Makowski.

1. Thornber, J. P. (1975) *Annu. Rev. Plant Physiol.* **26,** 127–158.
2. Arntzen, C. J. (1978) *Curr. Top. Bioenerg.* **8,** 111–160.
3. Chua, N.-H. (1980) *Methods Enzymol.* **69,** 434–446.
4. Schmidt, G. W., Bartlett, S. G., Grossman, A. R., Cashmore, A. R. & Chua, N.-H. (1981) *J. Cell Biol.* **91,** 468–478.
5. Coruzzi, G., Broglie, G., Cashmore, A. & Chua, N.-H. (1983) *J. Biol. Chem.* **258,** 1399–1402.
6. Cashmore, A. R. (1984) *Proc. Natl. Acad. Sci. USA* **81,** 2960–2964.
7. Chua, N.-H. & Blomber, F. (1979) *J. Biol. Chem.* **254,** 215–223.
8. Ryrie, I. J. (1983) *Eur. J. Biochem.* **131,** 149–155.
9. Arntzen, C. J., Armond, P. A., Briantais, J.-M., Burke, J. J. & Novitsky, W. P. (1976) *Brookhaven Symp. Biol.* **28,** 316–337.
10. Miller, K. R. (1976) *J. Ultrastruct. Res.* **54,** 159–167.
11. Andersson, B., Anderson, J. M. & Ryrie, I. J. (1982) *Eur. J. Biochem.* **123,** 465–472.
12. Burke, J. J., Ditto, C. L. & Arntzen, C. J. (1978) *Arch. Biochem. Biophys.* **187,** 252–263.
13. Steinback, K. E., Burke, J. J., Mullet, J. E. & Arntzen, C. J. (1978) in *Chloroplast Development,* eds. Akoyunoglou, G. & Akoyunoglou, G. (Elsevier, Amsterdam), pp. 389–400.
14. McDonnell, A. & Staehelin, L. A. (1980) *J. Cell Biol.* **84,** 40–56.
15. Mullet, J. E. & Arntzen, C. J. (1980) *Biochim. Biophys. Acta 589.* 100–117.
16. Li, J. & Hollingshead, C. (1982) *Biophys. J.* **37,** 363–370.
17. Kühlbrandt, W., Thäler, Th. & Wehrli, E. (1983) *J. Cell Biol.* **96,** 1414–1424.
18. Holser, W. T. (1958) *Z. Kristallogr.* **110,** 266–281.
19. Peterson, G. L. (1977) *Anal. Biochem.* **83,** 346–356.
20. Lowry, O. H., Rosebrough, N. J., Farr, A. L. & Randall, R. J. (1951) *J. Biol. Chem.* **193,** 265–275.
21. Arnon, D. I. (1949) *Plant Physiol.* **24,** 1–5.
22. Singleton, W. S., Gray, M. S., Brown, M. L. & White, J. L. (1965) *J. Am. Oil Chem. Soc.* **42,** 53–56.
23. Klein, R. A. (1970) *Biochim. Biophys. Acta* **210,** 486–489.
24. Ames, B. N. (1966) *Methods Enzymol.* **8,** 115–118.
25. Gerritsen, W. J., Verkleij, A. J., Zwaal, R. F. A. & van Deenen, L. L. M. (1978) *Eur. J. Biochem.* **85,** 255–261.
26. Holloway, P. W. (1973) *Anal. Biochem.* **53,** 304–308.
27. Wingfield, P., Talmon, A., Leonard, K. & Weiss, H. (1979) *Nature (London)* **280,** 696–697.
28. Amos, L. A., Henderson, R. & Unwin, P. N. T. (1982) *Prog. Biophys. Mol. Biol.* **39,** 183–231.
29. Arndt, U. W., Barrington-Leigh, J., Mallett, J. F. W. & Twinn, K. E. (1969) *J. Phys. E* **2,** 385–387.
30. Henderson, R. & Unwin, P. N. T. (1975) *Nature (London)* **257,** 28–32.
31. Shaw, P. J. & Hills, G. J. (1981) *Micron* **12,** 279–282.
32. Deatherage, J. F., Henderson, R. & Capaldi, R. A. (1982) *J. Mol. Biol.* **158,** 487–499.
33. Cohen, H. A., Jerry, T. W. & Chiu, W. (1982) *Fortieth Annual Proceedings of The Electron Microscopy Society American,* ed. Bailey, G. W. (Claitor, Baton Rouge), p. 80.
34. Fuller, S. D., Capaldi, R. A. & Henderson, R. (1979) *J. Mol. Biol.* **134,** 305–327.
35. Matthews, B. W., Fenna, R. E., Bolognesi, M. C., Schmid, M. F. & Olson, J. M. (1979) *J. Mol. Biol.* **131,** 259–285.
36. Nabedryk, E., Andrianambinintsoa, S. & Breton, J. (1984) *Biochim. Biophys. Acta* **765,** 380–387.
37. Steinback, K. E., Burke, J. J. & Arntzen, C. J. (1979) *Arch. Biochem. Biophys.* **195,** 546–557.
38. Mullet, J. E. (1980) Dissertation (Univ. of Illinois).
39. Kyte, J. & Doolittle, R. F. (1982) *J. Mol. Biol.* **157,** 105–132.